Interdependency between heart rate variability and sleep EEG: linear/non-linear?

Martine Dumont[a],*, Fabrice Jurysta[b], Jean-Pol Lanquart[b], Pierre-François Migeotte[c], Philippe van de Borne[d], Paul Linkowski[b]

[a]*Biological Physics Department, University of Mons-Hainaut, Place du Parc, Mons 7000, Belgium*
[b]*Sleep Laboratory, Department of Psychiatry, Erasme Academic Hospital, Free University of Brussels, Brussels, Belgium*
[c]*Biomedical Physics Laboratory, Free University of Brussels, Brussels, Belgium*
[d]*Department of Cardiology and Hypertension Clinic, Erasme Academic Hospital, Free University of Brussels, Brussels, Belgium*

Abstract

Objective: To investigate whether the interdependency between heart rate variability (HRV) and sleep electroencephalogram (EEG) power spectra is linear or non-linear.

Methods: Heart rate and sleep EEG signals were recorded in 8 healthy young men. Spectral analysis was applied to electrocardiogram and EEG sleep recordings. Synchronization likelihood was computed over the first 3 non-rapid eye movement–rapid eye movement sleep cycles between normalized high frequency of RR intervals (RRI) and all electroencephalographic frequency bands. Comparison to surrogate data of different types was used to attest statistical significance of the coupling between RRI and EEG power bands and its linear or non-linear character.

Results: Synchronization likelihood values were statistically greater than univariate surrogate synchronization for all sleep bands both at the individual and the group levels. With reference to multivariate surrogates, synchronization values were statistically greater at the group level and, in a majority of cases, for individual comparison except for σ and β bands.

Conclusions: While all electroencephalographic power bands are linked to normalized high frequency RRI band, this interdependency is non-linear for δ, θ and α bands.

Significance: Non-linear description is required to capture the full interdependent dynamics of HRV and sleep EEG power bands.
© 2004 International Federation of Clinical Neurophysiology. Published by Elsevier Ireland Ltd. All rights reserved.

Keywords: Synchronization likelihood; Heart rate variability; Non-linear analysis; Sleep

1. Introduction

Recent years have seen a growing interest in the interactions between heart rate variability (HRV) and electroencephalogram (EEG) during sleep with the aim of a better understanding of the complex brain systems implicated in different physiological phenomena which occur across the night such as reduction of blood pressure (Mancia, 1993; Somers et al., 1993) or myocardial infarctions (Somers et al., 1993; Vanoli et al., 1995). A large number of studies indicated that cardiac events predominate in the early morning hours (Muller et al., 1985, 1987; Pepine, 1991). This may be linked to the predominance of rapid eye movement sleep (REM) at the end of the sleep period. REM is associated with large fluctuations in blood pressure, heart rate and sympathetic activity (Somers et al., 1993; Vanoli et al., 1995; Vaughn et al., 1995) which could trigger cardiac events.

Several authors have focused their attention on the dynamic interaction between HRV and only one or two sleep EEG power bands (Ako et al., 2003; Brandenberger et al., 2001; Yang et al., 2002).

Recently, we investigated this interaction by a linear method computing the coherency and the gain between the normalized high frequency (HF$_{nu}$) of the RR interval (RRI) and each normalized sleep EEG power band (δ, θ, α, σ and β) across the first 3 NREM–REM cycles (Jurysta et al., 2003). In healthy humans, the high frequency spectral

* Corresponding author. Tel.: +32-65373462; fax: +32-65373537.
E-mail address: martine.dumont@umh.ac.be (M. Dumont).

component of RRIs, associated with fast oscillations displayed by the heart rate at the respiratory frequency, is a marker of the cardiac vagal activity (Task Force, 1996; Zemaityte et al., 1986). We reported high (>0.50) coherency values (ranging from 0.74 to 0.88) between each EEG power band and HF_{nu} and the highest gain between δ and HF_{nu}.

However, all these investigations describe relations between the investigated time series in a linear way and are not able to detect non-linear interdependencies. The question about non-linearity is justified when analyzing data related to brain or cardiac activity. Indeed the elementary elements of brain activity, i.e. neuron firing, are governed by non-linear law (e.g. see Freeman, 1975). Non-linear methods for the analysis of the dynamic interactions between two physiological signals have been applied by different authors in various fields such as the cardiovascular system (e.g. Nollo et al., 2002), cardiorespiratory system (e.g. Toledo et al., 2002), or brain activity during rest (e.g. Breakspear and Terry, 2002) and epilepsy (e.g. Altenburg et al., 2002; Arnhold et al., 1999; Le Van Quyen et al., 1999). Interactions during sleep were also investigated by non-linear methods (Pereda et al., 2001) but the interactions between each normalized sleep EEG power band (δ, θ, α, σ and β) and HF_{nu} of the RRI have not yet been studied.

The objective of the present paper is to investigate the nature of the dynamic interdependency between sleep power bands and the HF band of RRI. We proceeded to a further investigation of previously analyzed data (Jurysta et al., 2003) by computing the synchronization likelihood, which takes into account all kinds of interdependencies between two signals without restriction to linear interdependency (Stam and van Dijk, 2002). Our question is: 'Is the dynamic interaction between sleep EEG and HRV linear or non-linear?'

Synchronization likelihood is a measure of the degree of synchronization or coupling between two or more dynamic systems. It is based on the concept of generalized synchronization that exists between two dynamic systems X and Y if the temporal evolution of one of the systems (e.g. Y) is a continuous function F of the other (e.g. X). Contrary to the linear response methodology (gain and coherency), the relation between X and Y and thus F does not have to be linear. Contrary to identical synchronization, generalized synchronization does not require the time series to be identical but to be related by a continuous functional relationship.

Generalized synchronization has been applied to investigate interdependencies between systems of the same nature, such as between different EEG or MEG channel recordings (e.g. Arnhold et al., 1999; Breakspear and Terry, 2002; Le Van Quyen et al., 1999; Pereda et al., 2001). Investigation of structurally non-equivalent systems has been reported for chaotic models by Abarbanel et al. (1996), Boccaletti et al. (2000), and Le Van Quyen et al. (1999) and coupling between systems of different nature has been

studied for the cardiovascular (e.g. Nollo et al., 2002) and cardiorespiratory (e.g. Toledo et al., 2002) systems.

Until now, synchronization likelihood has been applied to the detection of coupling between systems of the same nature, i.e. EEG or MEG data (Altenburg et al., 2002; Stam et al., 2003). This study is the first application of this methodology to systems of a different nature such as heart and brain.

2. Methods

2.1. Subjects

Eight healthy young adult males aged between 18 and 23 years (mean 20.5) were recorded during 4 successive nights.

Each subject was given a detailed description and demonstration of the procedure and apparatus involved in the study before signing a consent form. The study protocol was approved by the local ethical committee of Erasme Academic Hospital.

These data were obtained during our previous study (Jurysta et al., 2003), where detailed information about the EEG and ECG recordings can be found. Subjects were not allowed to sleep during the day and were asked to retire around 11:00 p.m. They were left to awake spontaneously in the morning. No recording was carried out on the first night to allow the subjects to adjust to their surroundings. During the second night, polysomnography was performed to detect sleep pathologies such as apnea–hypopnea syndrome, periodic leg movement syndrome, parasomnia and snoring. On nights 3 and 4, ECG activity was recorded and polysomnography was performed with two electrooculo-gramms, 3 EEGs (Fz-Ax, Cz-Ax, Oz-Ax, where Ax was a mastoid reference) and one submental electromyogram.

Respiration frequency was not recorded because we have observed that changes in the respiration pattern during sleep contribute only modestly to the nocturnal changes in RRI variability (van de Borne et al., 1995). Thus it is unlikely that reduction in the HF variability of RRI due to irregular respiration interfered importantly with our measure of HF_{nu}.

2.2. Readings

From the last two night data we chose for analysis the night that did not show any visual or computed artifacts, selecting one at random if both nights were satisfactory. Each 20 s epoch was visually scored according to standard criteria (Rechtschaffen and Kales, 1968). The analysis was performed off-line on the first 3 NREM–REM cycles for comparison with our previous study (Jurysta et al., 2003) where the investigated time interval was necessarily reduced to satisfy the stationarity requirement of the linear investigation.

Fast Fourier transform (FFT) was applied to EEG recordings on each 5 s data window and the results were

averaged every 20 s. The power was grouped into 5 conventional bands: δ [0.5–3.0 Hz], θ [3.0–8.0 Hz] α [8.0–12.0 Hz], σ [12.0–16.0 Hz], and β [16.0–25 Hz]. The EEG spectral components were expressed in normalized units as the ratio between the power value and the full night mean power value in each specific frequency band (Aeschbach et al., 1997; Borbely et al., 1981). For the present analysis the Cz-Ax derivation was used.

The RRI time series were automatically computed and visually corrected from the QRS complexes. The spectral components—low frequency (LF) (0.04 Hz $< f <$ 0.15 Hz) and high frequency (HF) (0.15 Hz $< f <$ 0.40 Hz) of HRV—were computed according to the recommendations of the Task Force of the European Society of Cardiology and the North American Society of Pacing and Electrophysiology (1996) on 120 s windows. Shifting such 120 s window ahead by 20 s permits the computation of the spectral component each 20 s followed by normalization according to $LF_{nu} = LF/(LF + HF)$ and $HF_{nu} = HF/(LF + HF)$.

We thus obtained power values for the spectral components of both EEG and RRI bands every 20 s.

2.3. Synchronization likelihood

Of various methods of quantifying generalized synchronization such as those based on mutual neighbors (Arnhold et al., 1999) or mutual prediction (Breakspear and Terry, 2002; Pereda et al., 2001; Schiff et al., 1996) we chose to use the synchronization likelihood introduced by Stam and van Dijk (2002). It showed promising results when applied to MEG and EEG characterizations (Stam and van Dijk, 2002; Stam et al., 2003) and in epilepsy detection for newborns (Altenburg et al., 2002).

The synchronization likelihood between two dynamic systems X and Y represented by two simultaneously recorded scalar time series $\{x_i = x(t_i), \ 1 \leq i \leq \mathcal{N}\}$ and $\{y_i = y(t_i), \ 1 \leq i \leq \mathcal{N}\}$ is introduced briefly as follows.

If generalized synchronization holds then when system X is in two close states X_i and X_j at times t_i and t_j then system Y will be in close states Y_i and Y_j at the same times.

States of the system X are reconstructed in an m_x-dimensional phase space by the time delay method (Takens, 1981):

$$X_i = (x_i, x_{i+\tau_x}, x_{i+2\tau_x}, ..., x_{i+(m_x-1)\tau_x}), \ 1 \leq i \leq N_x \quad (1)$$

where τ_x is a time delay (an integer multiple of the sampling interval) and

$$N_x = \mathcal{N} - (m_x - 1)\tau_x \quad (2)$$

is the number of vectors in the reconstructed X phase space.

One proceeds similarly for the time series $\{y_i = y(t_i)\}$ with regards to reconstruction parameters m_y and τ_y. For synchronization likelihood computation we consider an equal number N of reconstructed vectors for each time series for example $N = \min(N_x, N_y)$.

Note that compared to Stam and van Dijk (2002)'s initial paper, we have extended the definition of the synchronization likelihood by considering different reconstruction parameters m_i and τ_i for each channel $i = x, y$, cf. Eq. (1), in view of the application to systems with different dynamic characteristics. Specific reconstruction parameters are also set up in other generalized synchronization measures such as Schiff et al. (1996) and Terry and Breakspear (2003).

The synchronization likelihood $S_{i,j}$ for a pair of times t_i and t_j is the probability of finding system Y at time t_j in a state Y_j close to its state Y_i at time t_i provided system X is in close states X_j and X_i at the same times t_j and t_i. The synchronization likelihood S_i at time t_i is obtained by averaging $S_{i,j}$ over times t_j.

Close states of the system X at times t_i and t_j are defined as close points X_i and X_j in the phase space Eq. (1) with respect to some cut off ϵ_i^X :

$$|X_i - X_j| < \epsilon_i^X \quad (3)$$

where $|\cdots|$ denotes the Euclidean distance.

The cut off ϵ_i^X is defined in such a way that the probability of finding a point X_j in X phase space within a distance ϵ_i^X from X_i is equal to some low value p_{ref} :

$$P_i(\epsilon_i^X) = \frac{1}{2(w_2 - w_1 - 1)} \sum_{\substack{j=1 \\ w_i < |i-j| < w_2}}^{N} \theta(\epsilon_i^X - |X_i - X_j|)$$

$$= p_{ref} \quad (4)$$

$\theta(x)$ stands for the Heaviside step function, $\theta(x) = 0$ for $x \leq 0$, $\theta(x) = 1$ for $x > 0$.

w_1 is the Theiler correction to avoid autocorrelation (Theiler, 1986). w_2 may be used to sharpen the time resolution of the synchronization search within a limited window and reduce the computation time, it may be set equal to the length of the time series too.

In the Y phase space points are qualified close with respect to a cut off ϵ_i^Y defined in a similar way to Eq. (4). The same probability value p_{ref} is used to define the cut off ϵ_i^X and ϵ_i^Y. p_{ref} represents the probability that one gets by chance points Y_i and Y_j close together when one has points X_i and X_j close together in case of two uncorrelated time series. p_{ref} hence controls for chance coincident events occurring between uncorrelated systems of (possibly) different complexity and dimensionality.

The synchronization likelihood S_i is computed as

$$S_i = \frac{1}{2(w_2 - w_1 - 1)p_{ref}} \sum_{\substack{j=1 \\ w_1 < |i-j| < w_2 \\ |X_i - X_j| < \epsilon_i^X}}^{N} \theta(\epsilon_i^Y - |Y_i - Y_j|) \quad (5)$$

where $2(w_2 - w_1 - 1)p_{ref}$ is the number of values of j satisfying the summation conditions (cf. Eq. (4)).

Averaging S_i over the time index i defines the synchronization likelihood S.

For uncorrelated systems $S_i = p_{ref}$ whereas for systems with complete synchronization $S_i = 1$.

The definition of the synchronization likelihood can be extended to M dynamical systems (Stam and van Dijk, 2002). Note that when evaluated between two channels X and Y the synchronization likelihood is symmetrical in X and Y and cannot help to determine which of the two systems is the driver. For that purpose asymmetric synchronization measures such as those proposed by Arnhold et al. (1999) or Terry and Breakspear (2003) should be used.

2.4. Surrogate data

To assess the statistical significance of the interdependency observed as well as its nature (linear or non-linear) we performed surrogate data testing with surrogates of different types (Prichard and Theiler, 1994; Schreiber and Schmitz, 2000; Theiler et al., 1992).

Surrogate data testing is hypothesis testing, with the null hypothesis a potential explanation for the data observed. Surrogate data are test data constructed to share some linear properties with the experimental data under examination, in agreement with the null hypothesis and to be otherwise random. A statistic, here the synchronization likelihood S, is computed from the original data S_{orig} and from surrogates S_{surr}. If the null hypothesis is true, then the surrogate procedure will not affect the values of the statistic. On the other hand, if the statistic is significantly modified for the surrogates, the null hypothesis can be rejected.

We tested two different null hypotheses corresponding to two different types of surrogates.

First, we tested the null hypothesis that the data are uncorrelated filtered gaussian noise. Test data are univariate surrogates preserving all the linear properties of X and Y systems (amplitude distribution and power spectrum) but devoid of any coherent phase relationship between X and Y so that all the dependencies of Y on X are not present in the surrogates of Y. A simple way to construct univariate surrogate data with the same power spectrum as the original data is to perform a Fourier transformation of the data, adding a random phase to each Fourier component. By an inverse Fourier transformation one gets the surrogates. Original data and surrogates differ only by a phase factor in their Fourier components and have thus the same power spectrum. Construction of such surrogates for each signal independent of the other assures any phase relationship eventually present in and between the original data is lost in the surrogates. The construction of surrogates that share both the amplitude distribution and the power spectrum of the original data, as we use in the present investigation, will not be presented here and is detailed in Schreiber and Schmitz (2000). We use the algorithm of Hegger et al. (1999).

If there is significant interdependency between time series, the value of the synchronization likelihood S will be expected to be significantly greater for the original data than for the univariate surrogates.

In this case, it would be of interest to test the nature of the interdependency and to test another null hypothesis specifying that the data behaves as linearly correlated stochastic systems. Corresponding test data are multivariate surrogates. They are random data sharing with the original data, both their individual linear properties such as autocorrelation and amplitude distribution and their cross-correlation, while any non-linear information both within and between time series is lost.

To generate multivariate surrogates with the same power spectrum and cross-correlations as the original data, one proceeds as in the case of univariate surrogates but adds the same random phase to the Fourier components of the analyzed time series. As the phase difference between the Fourier components of the surrogates is unchanged compared to original data, the cross spectrum remains unchanged.

Again we refer to Schreiber and Schmitz (2000) for the generation of multivariate surrogates preserving the amplitude distribution and power spectrum of the original data. Rejection of the null hypothesis indicates in this case that S is sensitive to non-linear coupling present in the analyzed data.

2.5. Statistical analysis

Comparison between original and surrogate values may be performed in two ways.

At the individual level, i.e. for one time series, an ensemble of n surrogates is constructed from the original data with respect to the null hypothesis, and a Z-score

$$Z = \frac{S_{orig} - \langle S_{surr} \rangle}{SD_{surr}} \tag{6}$$

is computed where $\langle S_{surr} \rangle$ and SD_{surr} are respectively the mean value and the standard deviation of S evaluated for the surrogates. Z is the number of standard deviation S_{orig} is away from $\langle S_{surr} \rangle$. If the S_{surr} values are normally distributed, the null hypothesis is rejected at a $P < 0.05$ level if $Z > 1.64$ for a one-sided test.

One-sided tests are performed when expecting the values for the surrogates to be smaller (larger) than the values for the original data. In the present case we were interested in showing that the synchronization likelihood is greater in the original data than in univariate surrogates or in linearly correlated surrogates. We verified that the surrogate values obey a normal distribution by applying a Kolmogorov–Smirnov test. As an illustration of this normal behavior we show in Fig. 1 a normal plot for S_{surr} between the δ sleep band and HF_{nu} for multivariate surrogates generated for one subject (n^r 3) of our sample (parameter values used for the S computation may be found in Section 3).
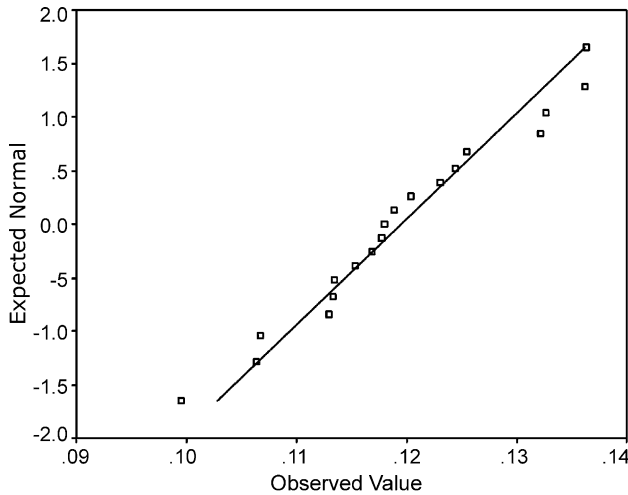
Fig. 1. Normal plot for S_{surr} between the δ sleep band and HF_{nu} for multivariate surrogates generated for subject 3.

At the group level, comparison can be statistically performed between the sample of S_{orig} from the original data and the sample of S_{surr} resulting from the generation of one surrogate per each original time series. Wilcoxon signed test or paired T test are the non-parametric and parametric tests, respectively, possibly used in that case, the null hypothesis being that the values of the two above-mentioned samples obey the same distribution. Our results refer to P-value < 0.05 and have been obtained both by Wilcoxon and paired T tests.

2.6. Choosing the reconstruction parameters

For the experimental data we chose the time delay τ_i for the phase space reconstruction Eq. (1) to be determined by one-fourth of the autocorrelation time τ_i^{ac}, where the autocorrelation time τ_i^{ac} is the time for which the autocorrelation function drops from initial value 1 to $1/e$ (Schiff et al., 1996). We then determined m_i by requiring the proportion of false nearest neighbor (FNN) to be smaller than 5% (Hegger and Kantz, 1999). Such a choice ensures that the reconstruction lengths $(m_i - 1)\tau_i$ are a small fraction of the NREM–REM cycle lengths.

We fixed w_1 at the maximum value of τ_i^{ac} for the different time series (δ, θ, α, σ, β and HF_{nu}) analyzed for each subject and for w_2 we used the length of the investigated time interval. We observed that the synchronization likelihood values depend weakly on the window w_1, w_2.

Note that FNN have less impact in the measurement of interdependency based on the synchronization likelihood than on the non-linear forecasting (e.g. see Breakspear and Terry, 2002) because synchronization likelihood is restricted to local investigation by use of the cut off ϵ_i^X, ϵ_j^Y fixed by a common probability level p_{ref} while forecasting is based on the future behavior of mutual neighbors, thus relying on nearest neighbor determination.

2.7. Tests

We tested the computation of the synchronization likelihood for a Lorenz model driven by the chaotic signal from a Rössler attractor (e.g. Le Van Quyen et al., 1999). The system dynamics is governed by differential equations. The Rössler systems is described by

$$\dot{x}_1 = -\alpha(x_2 + x_3)$$
$$\dot{x}_2 = \alpha(x_1 + ax_2) \tag{7}$$
$$\dot{x}_3 = \alpha(b + x_3(x_1 - c))$$

and the coupled Lorenz model by:

$$\dot{y}_1 = \sigma(y_2 - y_1)$$
$$\dot{y}_2 = -y_1y_3 + ry_1 - y_2 + Cx_2^2 \tag{8}$$
$$\dot{y}_3 = y_1y_2 - \beta y_3$$

where C is the strength of the unidirectional coupling and α is introduced to control the time scale of the driving system (we use $\alpha = 6$). $a = b = 0.2$, $c = 5.7$, $\sigma = 10$, $\beta = \frac{8}{3}$ and $r = 28$. Numerical integration was performed with a 4th order Runge–Kutta method and a time step $dt = 0.002$.

As an example, we report in Table 1 the synchronization likelihood S and the Z-score for $C = 8$ where generalized synchronization is observed in the auxiliary system approach (Abarbanel et al., 1996). The time series are the x_1 time series of the Rössler system reconstructed with $m_x = 3$, $\tau_x = 25$ and the y_1 time series of the Lorenz model reconstructed with $m_y = 6$, $\tau_y = 13$ for $C = 8$. $N = 4000$ points are used after first 2000 values have been discarded. The τ_i values are the first zero crossing of the corresponding autocorrelation functions, $m_x = 3$ and $m_y = 6$ are the real dimensions of the Rössler and coupled Lorenz state space. We also computed the synchronization likelihood between the same times series using common reconstruction parameters $m_x = m_y = 6$, $\tau_x = \tau_y = 25$. The synchronization window was chosen as $w_1 = \text{Max}(\tau_x, \tau_y)$, $w_2 = 400$. Whilst we get different values for S, we reach the same conclusion when testing against 19 surrogate data.

Table 1
Comparison between synchronization likelihood S computed with specific and common phase space reconstruction parameters for a Lorenz model driven by a Rössler attractor with $C = 0.8$

X	$m_x = 3, \tau_x = 25$	$m_x = 6, \tau_x = 25$
Y	$m_y = 6, \tau_y = 13$	$m_y = 6, \tau_y = 25$
S	0.403	0.388
Z_{uni}	9.00	10.59
Z_{multi}	3.11	2.45
$\text{Max}(S_{\text{surr}})_{\text{multi}}$	0.370	0.367
$\langle S_{\text{surr}}\rangle_{\text{multi}}$	0.317	0.319

τ_i and m_i specify the reconstruction parameter values. Z_{uni} and Z_{multi} denote the Z-score for univariate and multivariate surrogates, respectively. $\text{Max}(S_{\text{surr}})_{\text{multi}}$ and $\langle S_{\text{surr}}\rangle_{\text{multi}}$ stand for the maximum and mean values obtained for the multivariate surrogates.
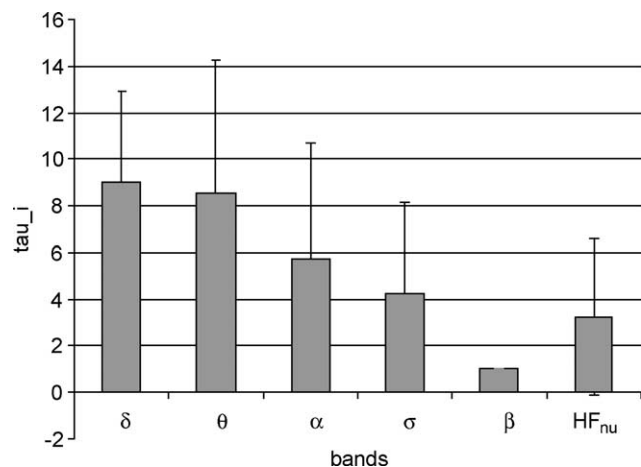
Fig. 2. Time delay τ_i, in unit of the sampling time of power spectra estimation. Bars show standard deviations. For β band, $\tau_\beta = 1$ for all subjects.

2.8. Softwares

HRV analysis and FFTs were performed with the software package MATLAB (The Math Works Inc., USA) and its signal processing toolbox (Matlab 6.1 with Signal Processing Toolbox 5.1).

We used the TISEAN (Hegger et al., 1999) package for surrogate generation, for false nearest neighbor determination and autocorrelation function computation. The synchronization likelihood and corresponding computation of Z-score were computed with Fortran programs developed by us. These Fortran codes have been tested on two coupled Henon attractors. Statistical analysis was performed with SPSS for Windows (SPSS 11.0.1, SPSS Inc., Chicago, IL, USA).
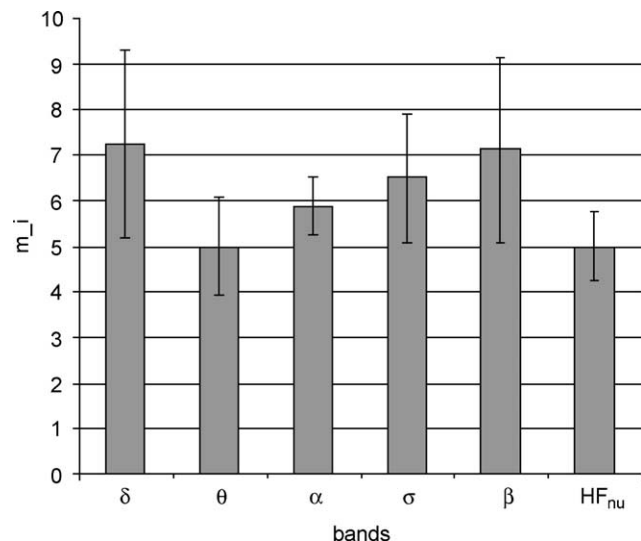

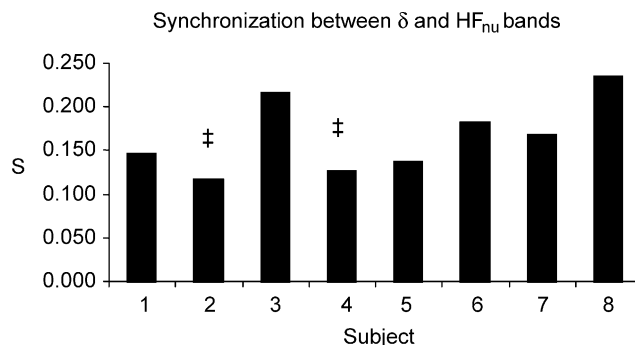Fig. 3. Phase space dimension m_i. Bars show standard deviations.

Fig. 4. Synchronization likelihood between sleep δ band and HF_{nu} band of HRV. ‡Subjects for which the null hypothesis of stochastic data with linear interdependencies is not rejected at a $P < 0.05$ level.

3. Results

We performed a synchronization likelihood computation between the different sleep bands and the HF_{nu} band of HRV. For statistical comparison, we proceed to the S computation for 19 surrogates of univariate and multivariate types.

We used the reconstruction parameters displayed in Figs. 2 and 3.

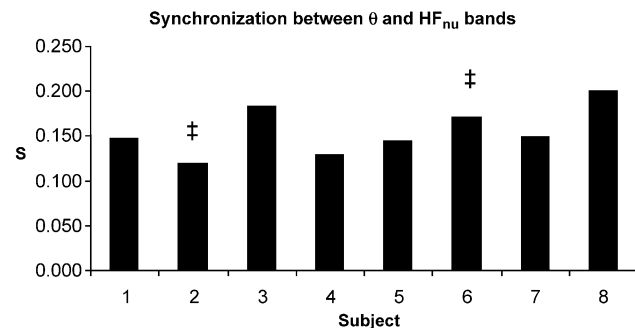Results corresponding to the synchronization of the δ band and the HF_{nu} of HRV indicate a clear sign of

Fig. 5. Synchronization likelihood between sleep θ band and HF_{nu} band of HRV. ‡Subjects for which the null hypothesis of stochastic data with linear interdependencies is not rejected at a $P < 0.05$ level.

Fig. 6. Synchronization likelihood between sleep α band and HF_{nu} band of HRV.

Fig. 7. Synchronization likelihood between sleep σ band and HF_{nu} band of HRV. ‡Subjects for which the null hypothesis of stochastic data with linear interdependencies is not rejected at a $P < 0.05$ level.
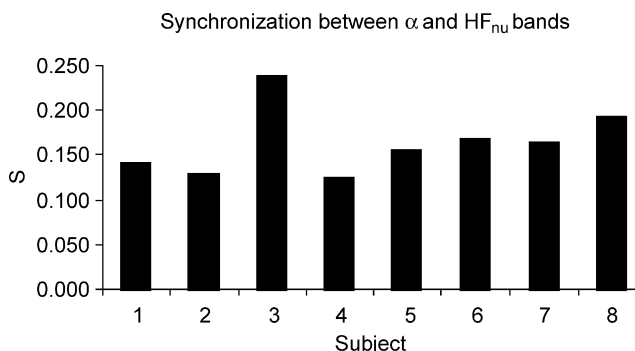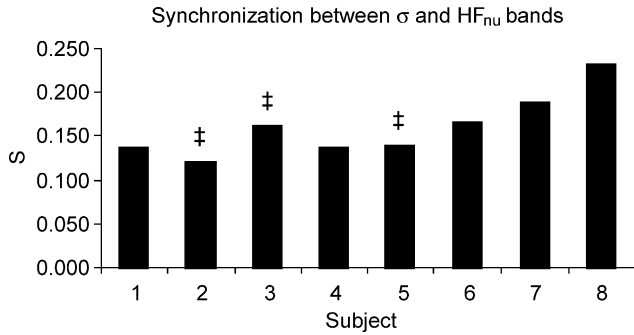

Fig. 8. Synchronization likelihood between sleep β band and HF_{nu} band of HRV. ‡Subjects for which the null hypothesis of stochastic data with linear interdependencies is not rejected at a $P < 0.05$ level.
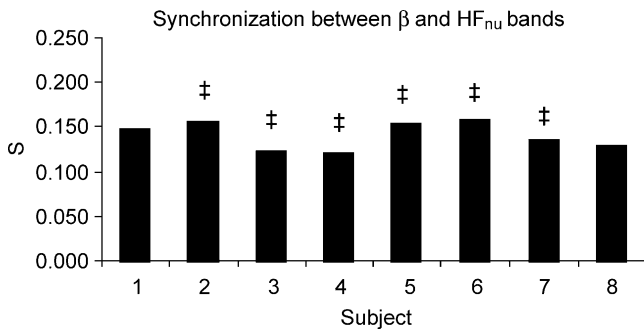
interdependency as the synchronization likelihood is greater than the value of $p_{ref} = 0.05$ corresponding to totally uncorrelated systems. We reached synchronization likelihood values ranging from 0.116 and 0.235 as shown in Fig. 4. Similar results were observed for the other sleep bands (see Figs. 5–8).

When testing against univariate surrogates at the individual level we could reject for any subject and any sleep band the null hypothesis of uncorrelated stochastic data at the $P < 0.05$ level. Rejection of this null hypothesis was also observed at the group level for any sleep band. This is in accordance with the linear analysis results showing that linear dependency exists between HF_{nu} and each sleep power band (Jurysta et al., 2003).

In any case, S statistically discriminates univariate and multivariate surrogates at the group level.

When testing against multivariate surrogate data at the individual level, the null hypothesis of stochastic data with linear interdependencies was rejected for six subjects for synchronization between HF_{nu} and the δ band. Rejection of this null hypothesis means that the data obey some non-linear interdependent dynamics. These results are illustrated in Fig. 4.

At the group level we rejected the null hypothesis of purely linear dependency with a $P < 0.05$ value. Corresponding values are reported in Table 2.

For the other sleep bands, we observed the same results as for δ, with a different number of subjects where the null hypothesis associated to multivariate surrogates cannot be rejected in individual testing. One should note that rejection for a subject in one band is not always associated with rejection for the other bands.

For the θ and σ bands we could reject the null hypothesis for 6 and 5 subjects, respectively, at the individual level. For the α band, rejection was obtained for all subjects and for the β band rejection was only observed in two subjects. These results are illustrated in Figs. 5–8. Note that a high value of S does not guarantee rejection of the null hypothesis (see e.g. subject 6 in Fig. 5). Rejection depends on the surrogate statistics for each subject.

At the group level, the null hypothesis of purely linear interdependency is rejected at a $P < 0.05$ level except for the σ and β bands. Corresponding results are collected in Table 2.

Table 2
Synchronization likelihood values between HF_{nu} and the different sleep bands for the original data S_{orig} and for one multivariate surrogate $S_{surr\text{-}multi}$, for each subject

Subject	δ		θ		α		σ		β	
	S_{orig}	$S_{surr\text{-}multi}$	S_{orig}	$S_{surr\text{-}multi}$	S_{orig}	$S_{surr\text{-}multi}$	S_{orig}	$S_{surr\text{-}multi}$	S_{orig}	$S_{surr\text{-}multi}$
1	0.146	0.121	0.147	0.129	0.141	0.108	0.136	0.120	0.148	0.124
2	0.116	0.120	0.120	0.115	0.129	0.121	0.120	0.151	0.156	0.195
3	0.216	0.100	0.183	0.107	0.237	0.193	0.162	0.202	0.122	0.182
4	0.126	0.130	0.129	0.122	0.125	0.114	0.137	0.117	0.120	0.146
5	0.137	0.131	0.145	0.108	0.155	0.106	0.139	0.151	0.153	0.177
6	0.181	0.130	0.171	0.153	0.168	0.136	0.166	0.136	0.157	0.153
7	0.167	0.124	0.149	0.113	0.164	0.124	0.189	0.170	0.135	0.197
8	0.235	0.155	0.201	0.148	0.193	0.129	0.231	0.102	0.129	0.114

4. Conclusions

In this paper, the question of the non-linearity of the interaction between the different sleep EEG power bands (δ, θ, α, σ and β) and HF_{nu} band of the RRI was investigated in healthy subjects by computation of the synchronization likelihood.

While the present investigation confirms that all sleep EEG power bands are linked to the HF_{nu} of the RRI in agreement with the results we obtained previously by linear methods (Jurysta et al., 2003), we show by appropriate surrogate data testing a non-linear interdependency between δ, θ and α EEG power bands and the HF_{nu} of RRI. However, although the non-linear interdependency was shown for the group under investigation, some subjects show only a linear interdependency.

Recently, several authors (Ako et al., 2003; Brandenberger et al., 2001; Yang et al., 2002) and our group (Jurysta et al., 2003) used linear methods as the correlation, the coherence or the gain computation.

The results determined which sleep EEG band mostly interacts with the HF_{nu} of the RRI. The phase shifts between the sleep EEG spectral power bands and the spectral components of the HRV were computed.

These investigations demonstrated the interactions between EEG power bands and HF_{nu} of the RRI to be maximum between the normalized sleep δ EEG band and the normalized HF_{nu} with a phase advance in favor of the cardiac component (Brandenberger et al., 2001; Jurysta et al., 2003).

Ako et al. (2003) and Yang et al. (2002) both performed a linear regression analysis between the instantaneous values of EEG and HRV indices. Yang et al. (2002) reported a negative correlation between δ power and LF/HF ratio.

Ako et al. (2003) confirmed the negative correlation of the δ band with LF/HF and found a negative correlation between δ and LF with an estimate of

$$\widehat{\mathrm{LF}}(t) = b\delta(t) + a, \quad b < 0 \tag{9}$$

One may be puzzled by a tentative comparison between the synchronization likelihood results and those we reported regarding linear spectral analysis (Jurysta et al., 2003). Indeed we reported high (>0.50) coherency values (ranging from 0.74 to 0.88) and we report here linear interdependency only between HF_{nu} and σ and β bands.

Gain and coherency determinations present some restrictions that we discussed in our previous publication (Jurysta et al., 2003). This methodology does not take into account any interaction between different frequency components of the signals.

Indeed one signal y (e.g. δ), considered as the output, is estimated as a linear filtered version of an input x (e.g. HF_{nu}) in the frequency domain (Chatfield, 1989) by

$$\hat{y}(f) = H(f)x(f) \tag{10}$$

This expression connects the Fourier components of the estimate $\hat{y}(f)$ of $y(f)$ and $x(f)$ at the same frequency f. The gain $G(f)$ is the absolute value of the transfer $H(f)$ as

$$H(f) = G(f)e^{i\phi(f)}$$

and $\phi(f)$ the phase.

Our previous investigation focused on the $f^* = f_{\mathrm{NREM-REM}}$ frequencies corresponding to the cross spectrum peak frequencies. The gain and coherency were thus computed at the frequency of most common activity within the two signals in the frequency domain. This procedure is equivalent to a reduction of the analyzed signals to their single Fourier component at f^*, for example for δ and HF_{nu}

$$\hat{\delta}(t) = \delta(f^*)\cos(f^*t + \phi(f^*)) \tag{11}$$

and

$$HF_{nu}(t) = HF_{nu}(f^*)\cos(f^*t) \tag{12}$$

where $\delta(f^*)$ and $HF_{nu}(f^*)$ are the Fourier components of the δ power and HF_{nu} band at frequency f^*. Clearly the δ power and the HF_{nu} band are not such simple signals.

In contrast, synchronization likelihood takes into account interdependency between all frequency components of the analyzed signals.

The studies of Ako et al. (2003) and Yang et al. (2002) used a simpler description than linear transfer methodology and synchronization likelihood. A Fourier transformation of Eq. (9) indicates that linear regression would be compatible with linear transfer (gain and coherency) in the absence of an independent term $a = 0$ in Eq. (9) and for a frequency independent transfer function $G(f) = $ constant. Although Eqs. (9) and (10) do not refer to the same variables, compatibility of these types of description is not expected.

Within this context of the investigation of linear/non-linear interdependency, let us stress that coherency estimates the reliability of the linearity between x and y with the hypothesis of a linear system contaminated by noise uncorrelated with the input x. If the residual between the output signal and its estimate $\hat{y}$ contains a non-linear dependence in x, coherency can no more be related to the residual power and loses its significance for linearity reliability estimation. Non-linear interdependency is not incompatible with high coherency values. Proofs of the linearity between input and output must be performed outside a linear response frame such as Eq. (10). With respect to gain and coherency, the interest of the present investigation is to identify whether linear transfer methodology misses or does not miss a non-linear contribution of the interdependency between EEG sleep bands and HF_{nu}. Our results, with reference to surrogate data for statistical significance, reject non-linear interdependency with HF_{nu} only for the σ and β bands.

The observed linear and non-linear interdependencies may be tentatively interpreted as follows.

Cerebral activity, which is measured by EEG and quantified by the spectral powers, comes from neuronal activity. Each neuron discharges, or not, due to the presence, or the absence, of an electrical stimulation. The neurons are grouped into different brain structures, such as thalamus, brain stem, etc. Each of these structures is connected to other cerebral structures by a dense network of axons. The same thalamic neurons can oscillate in the σ and the δ frequency ranges depending on their membrane potential (Merica and Blois, 1997). Their cell membranes become progressively hyperpolarized due to a decrease in the firing rates of the brainstem cholinergic and monoaminergic neurons concomitantly with the sleep depth. δ production requires a large corticothalamic circuit with activation and inhibition loops while σ is only produced by thalamic neurons, which are also synchronized by the cortical neurons (Merica and Blois, 1997). β waves are produced by multiple neuronal stems located in the rostral midbrain, bulbar reticular core and cholinergic pedunculopontine tegmental and laterodorsal nuclei which are closed to the autonomic vagal nuclei. These neuronal structures, which produce different kinds of waves, can be considered as oscillators.

The rhythm generation provided by multiple oscillators was studied by Chang et al. (2000) in a study about the stability of the output rhythm of the sympathetic oscillators, which are involved in the sympathetic regulation of vascular tone in a thermoregulatory system. They showed that the population metastability is achieved through linear and non-linear dynamic interactions between the periodic driving force and single sympathetic oscillators and suggested that the generation of a stable population rhythm can exist even in the absence of mutual entrainment of its constituents, and this allows the population to generate a stable and flexible patterned response (Chang et al., 2000).

In agreement with their principles, our results suggest that the non-linear interdependency describes oscillators that generate rapid and adaptative responses. The hypothesis that brain stem centers implied in the cardiac vagal control and the cerebral structures implied in the sleep generation are in relation, is supported by different authors (Benarroch, 1993; Murali et al., 2003). Therefore, we suppose that the brain structures that interact between each other by a non-linear link, either present a stronger coupling than the brain structures that interact by a linear coupling, or interact without any dominant rhythm. These suppositions are confirmed by the $\sigma - \delta$ relationship and the sleep β power production. δ wave production requires a large corticothalamic circuit with a lot of positive or negative loops while σ production is produced by thalamic neurons. β waves are produced by a large number of cerebral stem structures as we described above. The physiological differences in the production of δ and σ waves may be revealed by non-linear methods: a more complex system, such as the interaction between δ and HF$_{nu}$, requires a non-linear model while a more simplistic system (with less oscillators or synchronized oscillators), such as σ and HF$_{nu}$ interaction, is described by a linear model. The linear coupling between HF$_{nu}$ and β EEG band proposes that the vasomotor center stem stimulates the cerebral structures implicated in the β sleep generation without any retroaction and, moreover, that each of these β stems discharges independently of the other stems at different times. This could explain the linear coupling and the weak (absolute or relative by comparison with the other bands) power of the β band (Armitage, 1995; Tan et al., 2000).

In conclusion, this study confirms that all sleep EEG power bands are coupled to the HF$_{nu}$ band of RRI in healthy young subjects. Until now the nature of this interdependency has not been specified. By an original application of non-linear analysis, we report that the interaction between δ, θ and α bands and HF$_{nu}$ is non-linear. This observation might be of importance in any further modeling of the complex interaction between sleep and nocturnal cardiac activity.

Acknowledgements

References

Abarbanel H, Rulkov N, Sushchik M. Generalized synchronzation of chaos: the auxiliary system approach. Phys Rev E 1996;53:4528–35.

Aeschbach D, Matthews JR, Postolache TT, Jackson MA, Giesen HA, Wehr TA. Dynamics of the human EEG during prolonged wakefulness: evidence for frequency-specific circadian and homeostatic influences. Neurosci Lett 1997;239:121–4.

Ako M, Kawara T, Uchida S, Miyazaki S, Nishihara K, Mukai J, Hirao K, Ako J, Okubo Y. Correlation between electroencephalographic and heart rate variability during sleep. Psychiatry Clin Neurosci 2003;57(1):59–65.

Altenburg J, Vermeulen RJ, Strijers RLM, Fetter WPF, Stam CJ. Seizure detection in the neonatal EEG with synchronization likelihood. Clin Neurophysiol 2002;114:50–5.

Armitage R. The distribution of EEG frequencies in REM and NREM sleep stages in healthy young adults. Sleep 1995;18(5):334–41.

Arnold J, Grassberger P, Lehnertz K, Elger CE. A robust method for detecting interdependences: application to intracranially recorded EEG. Physica D 1999;134:419–30.

Benarroch EE. The central autonomic network: functional organization, dysfunction, and perspective. Mayo Clin Proc 1993;68(10):988–1001.

Boccaletti S, Valladeres D, Kurths J, Maza D, Mancini H. Synchronization of structurally nonequivalent systems. Phys Rev E 2000;61:3712–5.

Borbely AA, Baumann F, Brandeis D, Strauch I, Dietrich L. Sleep deprivation: effect on sleep stages and EEG power density in man. Electroencephalogr Clin Neurophysiol 1981;51:483–93.

Brandenberger G, Ehrhart J, Piquard F, Simon C. Inverse coupling between ultradian oscillations in delta wave activity and heart rate variability during sleep. Clin Neurophysiol 2001;112(6):992–6.

Breakspear M, Terry JR. Detection and description of non-linear interdependance in normal multichannel human EEG data. Clin Neurophysiol 2002;113:735–53.

Chang HS, Staras K, Gilbey MP. Multiple oscillators provide metastability in rhythm generation. J Neurosci 2000;20(13):5135–43.

Chatfield C. The analysis of time series, 4th ed. London: Chapman & Hall; 1989.

Freeman W. Mass action in the nervous system. New York: Academic Press; 1975.

Hegger R, Kantz H. Improved false nearest neighbour method to detect determinism in time series data. Phys Rev E 1999;60:4970–3.

Hegger R, Kantz H, Schreiber T. Practical implementation of nonlinear time series methods: the Tisean package. Chaos 1999;4:413–35. http://www.mpiks-dresden.mpg.de/tisean.

Jurysta F, van de Borne Ph, Migeotte P-F, Dumont M, Lanquart J-P, Degaute J-P, Linkowski P. A study of the dynamic interactions between sleep EEG and heart rate variability in normal young men. Clin Neurophysiol 2003;114:2146–55.

Le Van Quyen M, Martinerie J, Adam C, Varela F. Nonlinear analysis of interictal EEG map the brain interdependencies in human focal epilepsy. Physica D 1999;143:10–14.

Mancia G. Autonomic modulation of the cardiovascular system during sleep. N Engl J Med 1993;328(5):347–9.

Merica H, Blois R. Relationship between the time courses of power in the frequency bands of human sleep EEG. Neurophysiol Clin 1997;27(2):116–28.

Muller JE, Stone PH, Turi ZG, Rutherford JD, Czeisler CA, Parker C, Poole WK, Passamani E, Roberts R, Robertson T, et al. Circadian variation in the frequency of onset of acute myocardial infarction. N Engl J Med 1985;313(21):1315–22.

Muller JE, Ludmer PL, Willich SN, Tofler GH, Aylmer G, Klangos I, Stone PH. Circadian variation in the frequency of sudden cardiac death. Circulation 1987;75(1):131–8.

Murali NS, Svatikova A, Somers VK. Cardiovascular physiology and sleep. Front Biosci 2003;8:s636–52.

Nollo G, Faes L, Porta A, Pellegrini B, Ravelli F, Del Greco M, Disertori M, Antolini R. Evidence of unbalanced regulatory mechanism of heart rate and systolic pressure after acute myocardial infarction. Am J Physiol 2002;283:H1200–7.

Pepine CJ. Circadian variations in myocardial ischemia. Implications for management. J Am Med Assoc 1991;265(3):386–90.

Pereda E, Rial R, Gamundi A, Gonzalez J. Assessment of changing interdependencies between electroencephalograms using nonlinear methods. Physica D 2001;148:147–58.

Prichard D, Theiler J. Generating surrogate data with several simultaneously measured variables. Phys Rev Lett 1994;73:951–4.

Rechtschaffen A, Kales A. A manual of standardized terminology techniques and scoring system for sleep stages of human subjects.

Los Angeles: Brain Information Service/Brain research Institute, University of California; 1968.

Schiff SJ, Po P, Chang T, Sauer T. Detecting dynamical interdependence and generalized synchrony through mutual prediction in a neural ensemble. Phys Rev E 1996;54:6708–24.

Schreiber T, Schmitz A. Surrogate time series. Physica D 2000;142:346–82.

Somers VK, Dyken ME, Mark AL, Abboud FM. Sympathetic-nerve activity during sleep in normal subjects. N Engl J Med 1993;328(5):303–7.

Stam CJ, van Dijk BW. Synchronisation likelihood: an unbiased measure of generalized synchronisation in multivariate data sets. Physica D 2002;163:236–51.

Stam CJ, Breakspear M, van Cappellen van Walsum AM, van Dijk B. Nonlinear synchronization in EEG and whole-head MEG recording of healthy subjects. Hum Brain Mapp 2003;19:63–78.

Takens F. Detecting strange attractors in turbulence. Lect Notes Math 1981;898:366–81.

Tan X, Campbell IG, Palagini L, Feinberg I. High internight reliability of computer-measured NREM delta, sigma, and beta: biological implications. Biol Psychiatry 2000;48(10):1010–9.

Task Force of the European Society of Cardiology and the North American Society of Pacing and Electrophysiology, Heart rate variability. Standards of measurements, physiological interpretation, and clinical use. Eur Heart J 1996;17:354–81.

Terry JR, Breakspear M. An improved algorithm for the detection of dynamical interdependence in bivariate time-series. Biol Cybern 2003;88(2):129–36.

Theiler J. Spurious dimension from correlation algorithms applied to limited time series data. Phys Rev Lett 1986;34:2427–32.

Theiler J, Eubank S, Longtin A, Galdrikian B, Farmer JD. Testing for nonlinearity in time series: the method of surrogate data. Physica D 1992;58:77–94.

Toledo E, Akselrod S, Pinhas I, Aravot D. Does synchronization reflect a true interaction in the cardiorespiratory system? Med Eng Phys 2002;24(1):45–52.

van de Borne P, Biston P, Paiva M, Nguyen H, Linkowski P, Degaute J-P. Cardiorespiratory transfer during sleep : a study in healthy young men. Am J Physiol 1995;269(3 Pt 2):H952–8.

Vanoli E, Adamson PB, Ba-Lin, Pinna GD, Lazzara R, Orr WC. Heart rate variability during specific sleep stages. A comparison of healthy subjects with patients after myocardial infarction. Circulation 1995;91(7):1918–22.

Vaughn BV, Quint SR, Messenheimer JA, Robertson KR. Heart period variability in sleep. Electroencephalogr Clin Neurophysiol 1995;94(3):155–62.

Yang C, Lai C-W, Lai HY, Kuo TBJ. Relationship between electroencephalogram slow-wave magnitude and heart rate variability during sleep in humans. Neurosci Lett 2002;329:213–6.

Zemaityte D, Varoneckas G, Plauska K, Kaukenas J. Components of the heart rhythm power spectrum in wakefulness and individual sleep stages. Int J Psychophysiol 1986;4(2):129–41.